NACA RM A50L12

NACA

RESEARCH MEMORANDUM

PRELIMINARY INVESTIGATION OF THE DELAY OF TURBULENT FLOW SEPARATION BY MEANS OF WEDGE-SHAPED BODIES

By George B. McCullough, Gerald E. Nitzberg, and John A. Kelly

Ames Aeronautical Laboratory
Moffett Field, Calif.

NATIONAL ADVISORY COMMITTEE FOR AERONAUTICS

WASHINGTON
March 1, 1951

NATIONAL ADVISORY COMMITTEE FOR AERONAUTICS

RESEARCH MEMORANDUM

PRELIMINARY INVESTIGATION OF THE DELAY OF TURBULENT FLOW SEPARATION BY MEANS OF WEDGE-SHAPED BODIES

By George B. McCullough, Gerald E. Nitzberg, and John A. Kelly

SUMMARY

An experimental investigation of pyramidal, wedge-like bodies as devices for delaying separation of a turbulent boundary layer was undertaken. Tests of individual wedges on a large flat plate showed that, within certain limits, effective boundary-layer control could be obtained with wedges of different geometry, but that the drag of the wedges was high, making it desirable to keep the size of the wedges to a minimum.

Tests of multiple small wedges attached to a two-dimensional NACA 633-018 airfoil model showed that greater maximum lift was attained by placing the wedges well forward along the chord, and by allowing open spaces between adjacent wedges. The best arrangement found increased the maximum lift of the airfoil about 45 percent at the expense of doubling the zero-lift drag. Similar gains were achieved by the use of small, vane-type vortex generators at about half the cost in drag.

INTRODUCTION

This report is concerned with an attempt to control the growth of a turbulent boundary layer by means of wedge-shaped bodies similar to the one shown in figure 1. The method was suggested by consideration of the types of flow associated with the NACA submerged inlet (reference 1), and the vane-type vortex generators described in reference 2.

Studies of the flow in the NACA submerged inlet indicated that, although a pair of vortices existed in the lee of the divergent walls of the inlet, the principal mechanism exerting a thinning action on the boundary layer on the floor of the inlet was the lateral spreading of the flow caused by the divergent walls. Also, the United Aircraft Corporation has shown that a turbulent boundary layer can be re-energized by utilizing the circulation of trailing vortices shed from the tips of

small low-aspect-ratio wings to mix high-energy air from the outer flow with the low-energy air near the surface on which boundary-layer control is desired. It was reasoned that a wedge-shaped body would combine both flow mechanisms and have the additional advantage of discharging the oncoming boundary layer flowing up the ramp as a sheet of vorticity over the oblique edge of the wedge. The discharged sheet of vorticity would, in turn, roll up into a trailing vortex. Thus, the action of the wedge would be threefold, and was expected to exert a powerful control on boundary-layer growth.

The investigation, conducted in the Ames 7- by 10-foot wind tunnels, consisted of, first, an exploration of the flow associated with individual wedges when mounted on a flat plate, and, second, a determination of the effectiveness of multiple wedges for delaying separation of the turbulent boundary layer from the upper surface of a two-dimensional airfoil model.

NOTATION

The coefficients and symbols contained in this report are defined as follows:

b wing span, feet

c wing chord, feet

c_d average section drag coefficient, corrected for jet-boundary effect by the method of reference 3 $\left(\frac{\text{drag}}{qcb}\right)$

Δc_d incremental section drag coefficient [(c_d for airfoil with wedges) − (c_d for airfoil without wedges)]

c_l average section lift coefficient, corrected for jet-boundary effect by the method of reference 3 $\left(\frac{\text{lift}}{qcb}\right)$

c_m average section pitching-moment coefficient referred to the quarter chord, corrected for jet-boundary effect by the method of reference 3 $\left(\frac{\text{pitching moment}}{qc^2b}\right)$

ΔH local total-pressure decrement [(free-stream total pressure) − (local total pressure in boundary layer or trailing vortex)], pounds per square foot

[redacted]

P pressure coefficient $\left[\frac{(\text{local static pressure}) - (\text{free-stream static pressure})}{q}\right]$

q free-stream dynamic pressure, pounds per square foot

V free-stream velocity, feet per second

x distance from airfoil leading edge measured parallel to the chord line, feet

y distance measured normal to surface (both flat plate and airfoil), inches

z lateral distance measured parallel to leading edge of wedge, inches

α_o section angle of attack, corrected for jet-boundary effect by the method of reference 3, degrees

δ_f flap deflection, degrees

Γ circulation of the discharged vortex, feet squared per second

MODELS AND TESTS

Individual Wedges Mounted on a Flat Plate

The items investigated during the tests of individual wedges include the minimum ramp angle and the maximum divergence angle which would permit well-defined vortex flow, the circulation of the discharged vortex, the effect on the boundary layer of the flat plate, the drag of the wedges, and the effect of the ratio of wedge height to the initial thickness of the oncoming boundary layer.

Three models, of different ramp and divergence angles, used in this phase of the investigation were relatively large in order to facilitate flow-direction measurements in the wake of the wedges. Other wedges of about one-third the size of the large wedges were used in connection with total-pressure measurements near the surface. The wedges were mounted on a large flat plate which formed a dummy wall parallel with the real wall of the wind tunnel so that the boundary layer of the tunnel wall passed beneath the flat plate. The leading edges of the wedges were normal to the stream direction and one face was parallel with it as shown in figure 1.

Visual studies of the flow were made by means of tufts and smoke filaments emitted from a row of orifices along the oblique edges of the various wedges. Other orifices installed in the wedges and in the wall permitted the measurement of pressure distribution. Surveys of the flow in the vicinity of the wall were made with small rakes of total-pressure tubes. In order to determine the circulation of the discharged vortex, maps of the flow velocity through a cross section of the wake downstream of the wedges were made using a previously calibrated four-pronged yaw head for determining flow direction. A photograph of the yaw head is shown in figure 2. The flow velocity was determined by means of a total- and a static-pressure tube mounted parallel with the axis of the yaw head. The offset of the static tube was taken into account in the calculation of the local flow velocity.

Most of the tests were made with free-stream dynamic pressures of 25 and 50 pounds per square foot. The smoke observations, however, necessitated a much lower speed.

Multiple Wedges Mounted on an Airfoil

The airfoil model employed in the investigation of multiple wedges was a 5-foot-chord, NACA 63_3-018 airfoil. When mounted in the wind tunnel, the model spanned the 7-foot dimension. Attached to the ends of the model were circular plates, 6 feet in diameter, which formed part of the tunnel floor and ceiling. The model was provided with a row of pressure orifices along the midspan section and a 27-1/2-percent-chord plain flap hinged on the chord line.

Several arrangements and chordwise locations of small wedges on the upper surface of the airfoil model were investigated briefly. All the tests, for which data are shown, were made with a basic wedge 9 inches long, 1 inch high, and with a divergence angle of 15°. Various combinations of wedges were produced using right-hand and left-hand wedges. (The wedge shown in fig. 1 was considered to be right hand.) The ramp angle was increased by piling one wedge on top of another. The wedge directly in contact with the airfoil was contoured to fit the surface. The particular arrangement of right-hand wedges shown in figure 3 was selected for more detailed study. These wedges were 2 inches high at the trailing edge so that the average ramp angle was about 12.5°.

The data obtained include the lift, drag, and pitching-moment characteristics as determined from the wind-tunnel balance system,[1] visual

[1]The data from the balance system include the unknown lift, drag, and pitching-moment tares of the circular plates on the ends of the model. Previous investigations have shown the lift and pitching-moment tares to be small.

observations of tufts, the chordwise distribution of pressure, and surveys of the flow adjacent to the surface. The tests were made with a dynamic pressure of 40 pounds per square foot which corresponds to a Reynolds number, based on the 5-foot-chord dimension, of 5,800,000.

RESULTS OF TESTS OF INDIVIDUAL WEDGES

Visual-Flow Studies

Photographs of the flow, as indicated by smoke filaments and by tufts, are shown in figure 4. The ramp angle of this wedge was 7°, and the angle of divergence 30°. The upper photograph shows that the boundary layer flowing over the oblique edge of the wedge was rolled up into a vortex and discharged near the trailing edge of the wedge. (The dark area beneath the helical smoke pattern was painted on the wall to provide visual contrast.) The spreading of the flow close to the wall is better shown in the accompanying tuft photograph.

It was found that as the angle of divergence was increased beyond about 50° the vortex flow persisted only part way along the oblique face of the wedge, then broke away and passed downstream. Behind the remainder of the face the flow eddied unsteadily. As the angle of divergence was decreased by rotating the wedge, the vortex remained visible until the angle approached zero. With the ramp angle reduced to 4°, only a portion of the smoke was entrained in the vortex; the remainder drifted over the region occupied by the vortex and mingled with the general flow.

Pressure Distribution

The distribution of static pressure on the inclined ramp and on the oblique face of the wedges, as well as on the wall downstream of the wedges, was determined from three streamwise rows of flush-type orifices. Data for the wedge shown in figure 4 are presented in figure 5. Similar pressure distributions were obtained for the other wedges.

The pressure diagrams were integrated and a pressure drag coefficient based on the projected frontal area of the wedges was computed. The value of the drag coefficient was about 0.3 for the wedge shown in figure 4. Reducing either the ramp angle or the angle of divergence reduced the drag coefficient. For a wedge with a ramp angle of 6° and a divergence angle of 15° the value of the drag coefficient was about 0.12.

Circulation Measurements

Attempts were made to determine the circulation of the vortices generated by three different wedge shapes by means of surveys of the flow. This proved to be a tedious undertaking because the flow angularities encountered exceeded the range of sensitivity of the yaw head and necessitated frequent stoppage of the wind tunnel to aline the survey device more nearly parallel with the local flow direction. Because of possible errors introduced by these readjustments, and also because of flow fluctuations, the measurements of circulation are considered to be only approximate (probably no better than ±5 percent), but the relative values determined for the various wedges are considered to be qualitatively correct at least.

Results of the drag and circulation measurements of the three wedges are given in the following table:

Wedge		$\frac{\Gamma}{V}$	Pressure-drag coefficient
Ramp angle (deg)	Divergence angle (deg)		
7	30	0.86	0.29
4	30	.45	.18
6	15	.34	.12

It will be noted that both the strength of the discharged vortex and the drag were lowered by reducing either the ramp angle or the angle of divergence. Increasing the displacement thickness of the boundary layer on the wall immediately ahead of the 7° wedge from 0.2 inch to 0.5 inch had little effect on the vortex strength or the drag.

Surveys of the flow in the vicinity of several wedges were made with a rake of total-pressure tubes which was moved laterally through the wake. Because the flow direction varied with distance away from the wall, some of the tubes of the rake were so oblique to the flow as to be unable to indicate the true total pressure, but, since the region immediately adjacent to the surface was of greatest interest, the rake was alined in the direction indicated by a tuft attached to the wall at each of the several positions occupied by the rake. In some locations, therefore, the surveys cannot be considered as boundary-layer surveys, but serve only to give a qualitative representation of the nature of the flow.

In figure 6 are shown contour maps derived from surveys made behind a small wedge of 6° ramp angle and 15° angle of divergence. The surveys were made at four stations, one-half, one,[2] two, and three wedge lengths downstream of the trailing edge of the wedge. The data are shown in the form of contours of constant values of the parameter $(1 - \Delta H/q)$. The vertical scale of the maps has been magnified two and one-half times to give more spread to the contours. Also shown on the maps are outline drawings of the wedge, and the contours of $(1 - \Delta H/q)$ for the bare wall. Although the data are only approximately correct, particularly at a distance from the wall because of angularities of the local flow mentioned previously, the low total-pressure region of the core of the vortex and the distortion of the boundary layer on the wall are clearly apparent. Also, the lateral shift of the center of the vortex with increasing distance downstream may be seen in this figure.

Similar, although less complete, surveys were made for the large wedges. The boundary layer along the ramp of the 7° wedge was approximately 1-1/2 inches thick. Behind the wedges the lateral distribution of total pressure was similar to that shown in figure 6. The minimum height of the $(1 - \Delta H/q) = 1$ contour at a lateral station one-third wedge length downstream of the trailing edge of the 7° wedge was about 1/4 inch; the corresponding height on the bare wall was 2 inches.

Reducing the ramp angle from 7° to 4° had little effect on the minimum height of the layer of reduced total pressure in spite of the reduced strength of the trailing vortex, but did reduce the lateral extent of the thinned-out layer. Reducing the angle of divergence from 30° to 15° approximately doubled the minimum thickness of the layer. Reducing the size of the wedge to one-third of its original dimensions without otherwise altering its geometry had little effect on the minimum thickness.

RESULTS OF TESTS OF MULTIPLE WEDGES

The first arrangement of wedges to be investigated on the airfoil model employed right-hand wedges adjoining one another so that the leading edges of the wedges formed a continuous straight line; thus giving a maximum number of trailing vortices (all rotating in the same sense).

Effect of Wedges on Maximum Lift

Chordwise location.- The variations of maximum section lift coefficient with chordwise location for wedges 1 inch and 2 inches high are

[2]Data for the right-hand half of this station were obtained by interpolation between data obtained one-half and two wedge lengths downstream.

[redacted]

shown in figure 7. The greatest average section lift coefficient obtained in this series of measurements was 1.85 for wedges 2 inches high with their leading edges at 25-percent chord. (The maximum section lift coefficient of the basic airfoil was 1.33.)

A similar series of measurements was made using right- and left-hand wedges alternately. The number of trailing vortices was the same as for the previous arrangement, but the sense of adjacent vortices alternated. The results of these measurements are also shown in figure 7. The maximum lifts obtained with the 1-inch-high wedges was about the same as with the arrangement employing right-hand wedges only, but with the alternating 2-inch-high wedges the maximum lifts were less than with the 2-inch-high right-hand wedges.

A few tests were made with wedges 3 inches high, but in each case the maximum lift was less than with the corresponding arrangement of wedges 2 inches high.

Wedge spacing.- The next variable investigated was that of wedge spacing. It was found that greater maximum lift was obtained with an open space between adjacent wedges, and that an open space equal to one wedge width was about optimum for this type of wedge. Since the data for figure 7 showed that it was advantageous to use a more forward location of the wedges, the tests with spaces between the wedges were made with the leading edges at 10- and 25-percent chord only. The greatest maximum average section lift coefficient obtained was 1.93 for 2-inch-high right-hand wedges spaced one wedge width apart with their leading edges at 10-percent chord. This is the configuration shown in figure 3, and was the one adopted for more extensive study.

Several wedge arrangements other than those mentioned were investigated briefly. Most of these were inferior to the configuration adopted for detailed study; others produced as much maximum lift with less drag, but the results were not consistently repeatable. It was concluded that they were too sensitive to small random flow disturbances to merit further consideration for this application.

Effect of Wedges on Drag

The difference in the drag coefficient (based on wing area) at zero lift for the airfoil with and without wedges is shown in figure 8 for the arrangements employing right-hand wedges for which maximum lift data are presented in figure 7. The incremental drag coefficient produced by the 1-inch-high wedges at 55-percent chord is about the same as the pressure drag coefficient, adjusted to wing area, measured for a geometrically similar wedge on the dummy wall. Doubling the height of

[redacted]

the wedges more than tripled the incremental drag. This would be expected from the drag data obtained for the individual wedges which showed that the drag coefficient based on frontal area was nearly proportional to the ramp angle or height of the wedges. Thus, doubling the wedge height would quadruple the value of an incremental drag coefficient based on wing area. The rapid rise of drag with forward movement of the wedges may be, in part, caused by the forward movement of transition from laminar to turbulent flow. Removing every other wedge reduced the incremental drag of the model nearly by half, and, as previously mentioned, actually benefited the maximum lift of the wing with 2-inch-high wedges.

Lift, Drag, and Pitching-Moment Characteristics of Configuration Adopted for Detailed Study

In figure 9 are shown the lift, drag, and pitching-moment characteristics of the airfoil with 2-inch-high wedges spaced one wedge width apart across the span at the 10-percent-chord station. Data are shown for the model with the trailing-edge flap set at various deflections from 0° to 40°. Similar data for the model without wedges are also presented. It should be remembered that the section drag coefficient includes the tare drag of the circular end plates.

The maximum section lift coefficient with the flap undeflected was increased from 1.33 to 1.93, an increase of 0.60. With the flap deflected 40°, the increase was from 2.07 to 2.39, or an increment of 0.32. The effect on the lift curve was to extend its nearly linear range to higher angles of attack. There was little effect on the angle for zero lift or on the lift-curve slope. With the flap deflected 20°, the shift of the lift curve caused by stalling of the flap was delayed to a higher angle of attack. With the flap deflected 40°, the flap was always stalled in the positive lift range, which probably accounts for the reduced effectiveness of the wedges.

The drag of the airfoil in the low and moderate lift range was, of course, greater with the wedges than without. In the high lift range corresponding to separated flow on the basic airfoil, however, the drag of the airfoil with wedges was less than the drag of the basic airfoil.

The zero-lift pitching moments were not significantly affected by the presence of the wedges, particularly for the airfoil with the flap undeflected. For a flap deflection of 20° the airfoil without wedges suffered a reduction in longitudinal stability, but this reduction was delayed to a higher angle of attack by the addition of wedges.

[redacted]

Flow Studies

Tufts.– Observations of tufts attached to the airfoil without wedges showed that the basic airfoil stalled from separation of the turbulent boundary layer. The separated area appeared initially at the trailing edge for an angle of attack of about 9°, and progressed steadily forward to about midchord at maximum lift. With the wedges in place, the initial appearance of separation was delayed to an angle of attack of about 20°. At higher angles of attack the flow was unsteady. The area of separation swept forward intermittently from the trailing edge to the position of the wedges, causing the airfoil model to lunge as the flow separated and reattached. At no time did the flow ahead of the wedges separate from the surface.

Pressure distribution.– In figure 10 are shown chordwise distributions of pressure on the airfoil with and without wedges. The angle of attack was 14.7°, corresponding to $c_{l_{max}}$ of the basic airfoil. Flow separation is indicated over the rear half of the basic airfoil by the region of relatively constant pressure, but for the airfoil with wedges the flow is attached as is shown by the continual recovery of pressure. A localized area of low pressure occurred in the vicinity of the wedges. (The line of pressure orifices passed through the center of an open space between wedges.)

For higher angles of attack the peak negative pressure near the nose of the airfoil continued to rise. For an angle of attack of 19.4° the pressure coefficient P attained a value of at least −11.5 without indication of flow separation at the trailing edge. Because of unsteadiness of flow, satisfactory pressure measurements could not be made at maximum lift.

Total-pressure surveys.– Total-pressure surveys were made at several chordwise stations downstream of the wedges. In figure 11 are shown the results of surveys made at the 95-percent-chord station for four angles of attack. These data are shown as contour maps of the parameter $(1 - \Delta H/q)$ similar to the maps in figure 6. The outline of the wedges in the figure appear distorted because of the magnified vertical scale. Similar data for the basic airfoil (except for 14.7° angle of attack for which angle the flow had separated from the surface) are also shown. The result of the action of the wedges as injectors of high-energy air into the thick turbulent boundary layer is apparent.

Test With Multiple Small Vanes

A brief investigation was made of vortex generators. These devices consisted of small vanes made of flat, 1/32-inch sheet brass as shown in the following sketch.

[redacted]

The vanes were installed 4-1/2 inches apart across the span of the airfoil model at the 10-percent-chord station. The angle of attack of the vanes was 22-1/2° with the sense of the angle of attack alternated between adjacent vanes so as to produce oppositely rotating trailing vortices. Lift, drag, and pitching-moment data for the model with the vane-type vortex generators are shown in figure 12. Also shown are similar data (from fig. 9) for the basic airfoil and the airfoil with wedges. The maximum lift coefficient with the vortex generators was 1.89, only 0.04 less than the maximum obtained with wedges.

Dimensions in inches

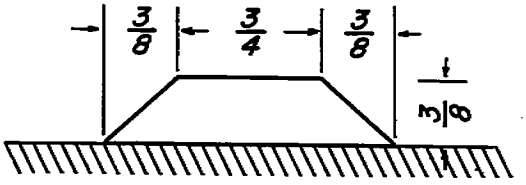

DISCUSSION

The tests of wedge-shaped bodies demonstrated that they did delay separation of the turbulent boundary layer from the surface of an airfoil. The relative importance of the roles played by the simple lateral spreading of the flow engendered by the diverging face of the wedge and by the induction of high-energy air into the boundary layer downstream of the wedges by the circulation of the trailing vortex was not made clear. The effectiveness of this latter mechanism depends on the distance of the axis of the vortex above the surface and on the diameter of the core, as well as on the circulation of the vortex. It is apparent that greater mixing action in the boundary layer would be realized if the axis of the vortex were brought down close to the vicinity of the outer edge of the boundary layer, and if the core diameter were reduced. In the present tests, the vane-type vortex generators were superior to the wedges in regard to both these effects.

The lesser effectiveness of the 1-inch-high wedges as compared to the 2-inch-high wedges (fig. 7) may be accounted for by the reduced ramp angle of the forward part of the wedge caused by contouring the lower surface to fit the surface of the airfoil. When mounted well forward on the wing, the average ramp angle of the forward half of the 1-inch-high wedges was about 3°. The tests on the dummy wall showed that the wedges were less effective when the ramp angle was reduced to 4°. The addition of the second wedge to make the total height 2 inches increased the ramp angle of the forward portion of the wedge to about 9°.

[redacted]

The reason for the failure of the maximum lift to increase when the closely spaced, 2-inch-high wedges were moved forward from the 25-percent-chord station to the 10-percent-chord station was not made clear. It is believed that the slightly blunt edges of the closely spaced wedges, when placed in the thin boundary layer near the leading edge, may have caused a sufficiently large local disturbance to precipitate flow separation.

The lesser effectiveness of the adjoining wedges as compared to the open-spaced wedges, in spite of the fact that the former arrangement produced twice as many vortices per unit span, may be due to the presence of a dead-air region in the angular space between the adjoining wedges. Such a dead-air region would accelerate boundary-layer growth and the occurrence of flow separation.

The drag of the wedges was shown by the tests on the dummy wall to be high. When the wedges are applied to a wing, the drag of the wing will be increased not only by the pressure and friction drag of the wedges themselves, but also by the increased friction drag of the wing resulting from the wedges fixing transition at a more forward station than normal. The high drag of the wedges makes it seem obvious that for any practical application they must be retracted into the wing for high-speed and cruising flight.

CONCLUDING REMARKS

The best arrangement of wedges applied to the NACA 63_3-018 airfoil model in the present investigation increased the maximum average lift coefficient from 1.33 to 1.93, an increase of 45 percent. With the plain flap deflected, the wedges also increased maximum lift, but the increment was not as great. The incremental drag coefficient caused by the wedges was about 0.006 in the low and moderate lift range. In the high lift range the drag of the wing with wedges was less than the drag of the plain wing.

A brief investigation of vane-type vortex generators applied to the NACA 63_3-018 airfoil model showed increments of maximum lift nearly as great as those produced by the wedges with about one-half the incremental drag. Apparently the mixing action of the smaller vortex generators is as effective as the combined flow mechanisms of the wedges.

Ames Aeronautical Laboratory,
National Advisory Committee for Aeronautics,
Moffett Field, Calif.

[redacted]

REFERENCES

1. Dryden, Hugh L.: 37th Wilbur Wright Lecture: The Aeronautical Research Scene – Goals, Methods, and Accomplishments. The Journal of the Royal Aeronautical Society, July 1949, v. 53, no. 463, pp. 623–666.

2. McCurdy, W. J.: Investigation of Boundary Layer Control of an NACA 16–325 Airfoil by Means of Vortex Generators. United Aircraft Corporation Research Department Report M–15038–3. Dec. 3, 1948.

3. Allen, H. Julian and Vincenti, Walter G.: Wall Interference in a Two–Dimensional–Flow Wind Tunnel with Consideration of the Effect of Compressibility. NACA Rep. 782, 1944.

[redacted]

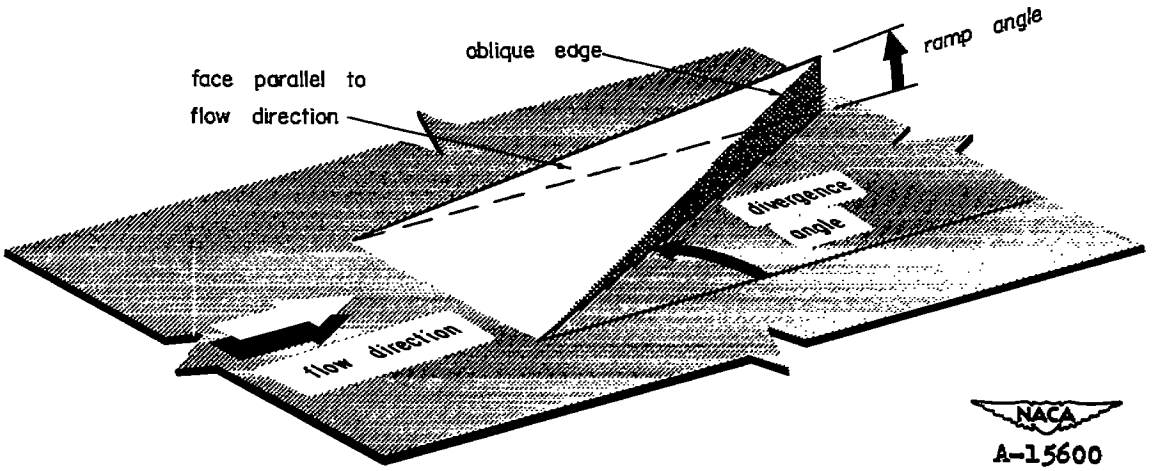

Figure 1.— Geometry and orientation of a typical wedge.

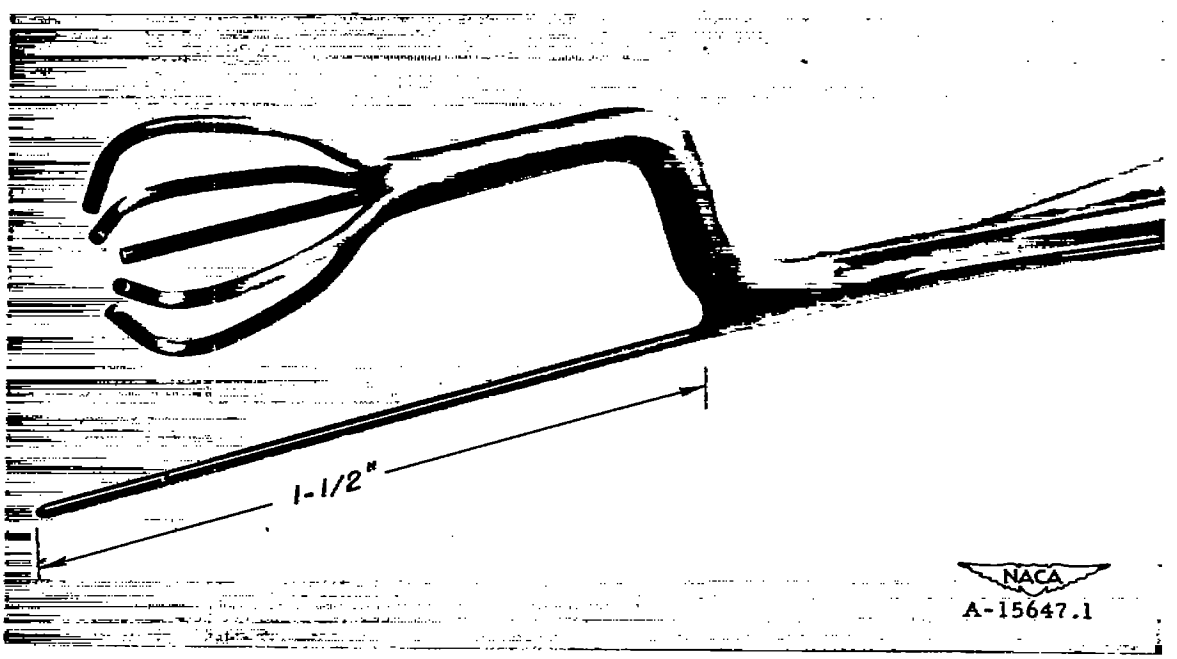

Figure 2.— Photograph of the four-pronged yaw head.

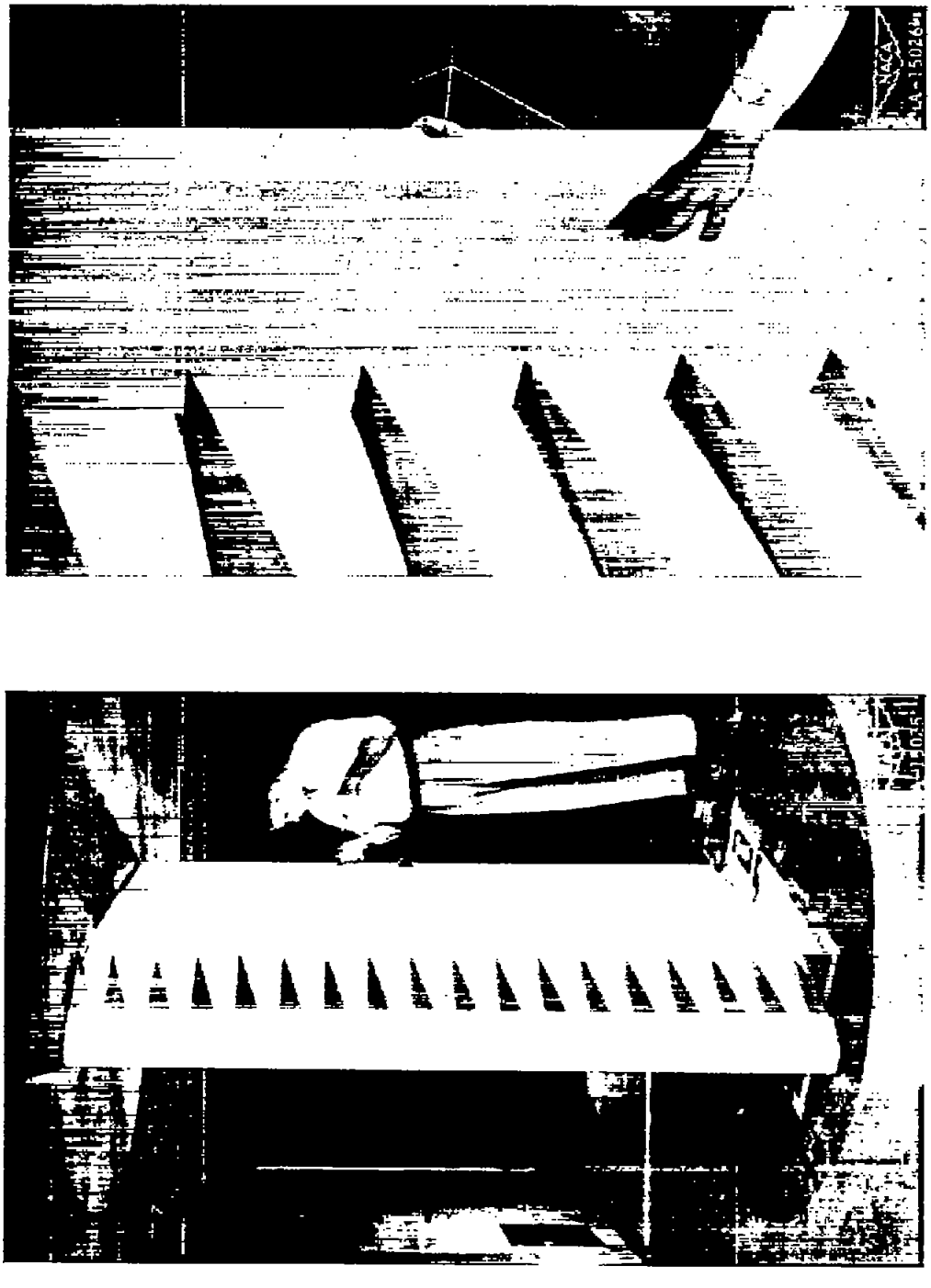

Figure 3.- Wedges mounted on NACA 63-018 airfoil model.

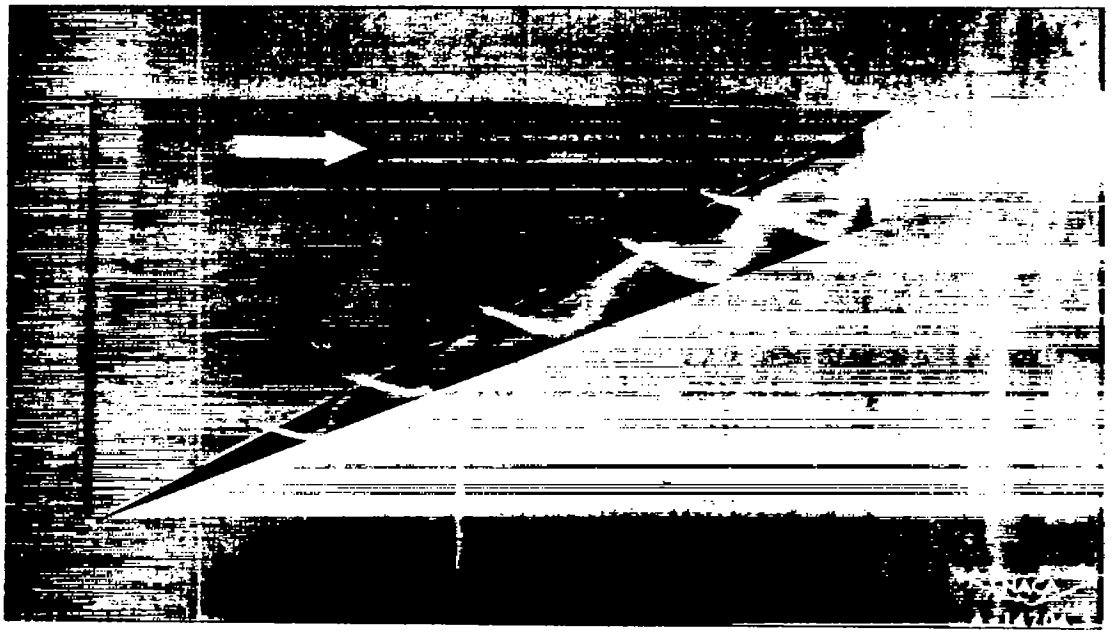

(a) Smoke study.

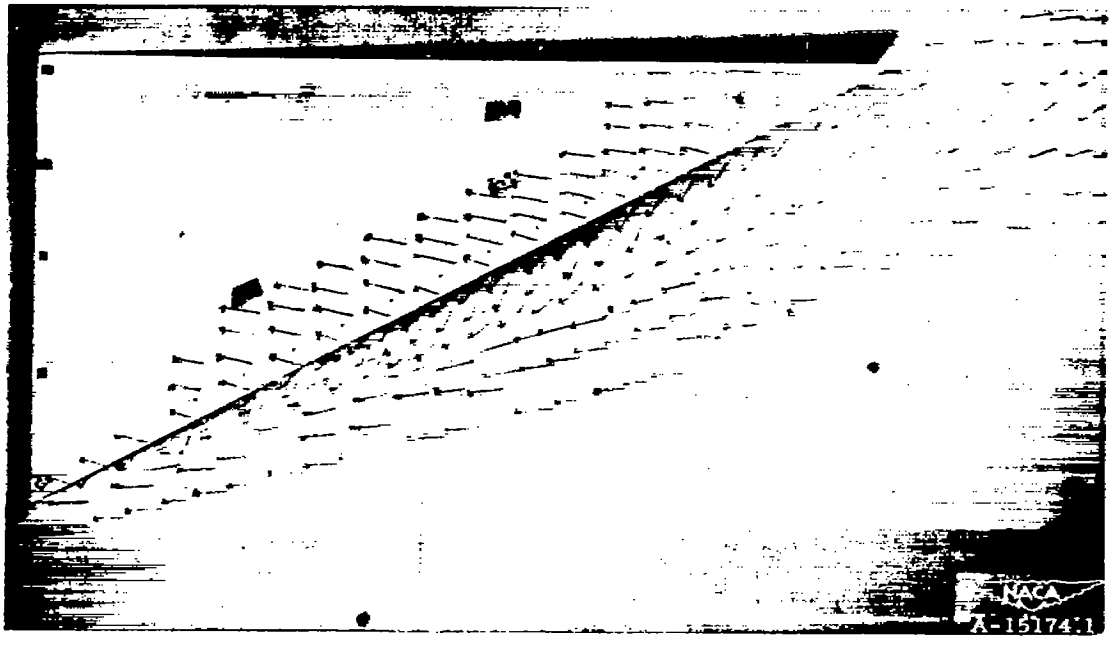

(b) Tuft study.

Figure 4.– Flow studies of large wedge mounted on flat plate.

[redacted]

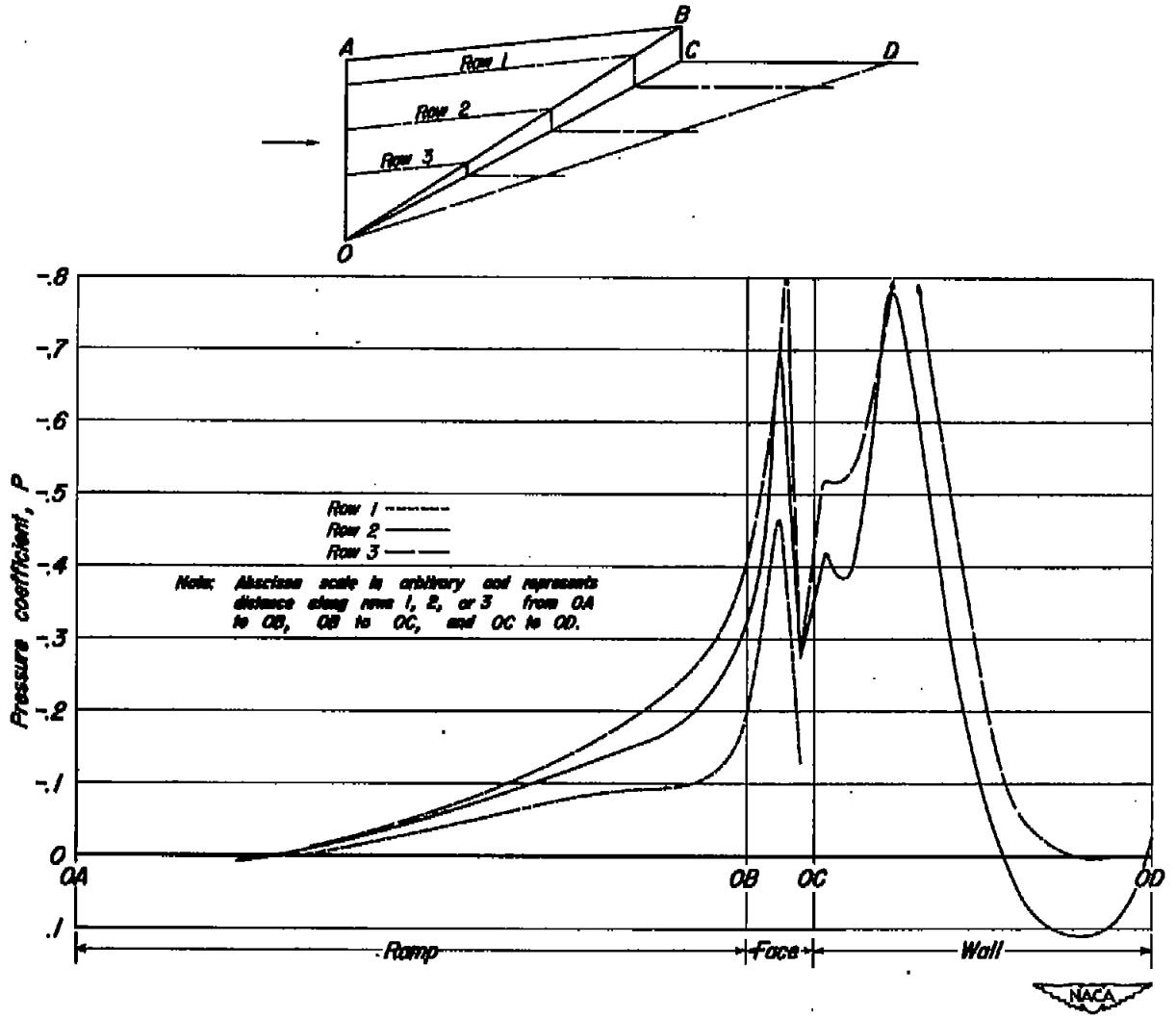

Figure 5.- Pressure distribution over a typical wedge.

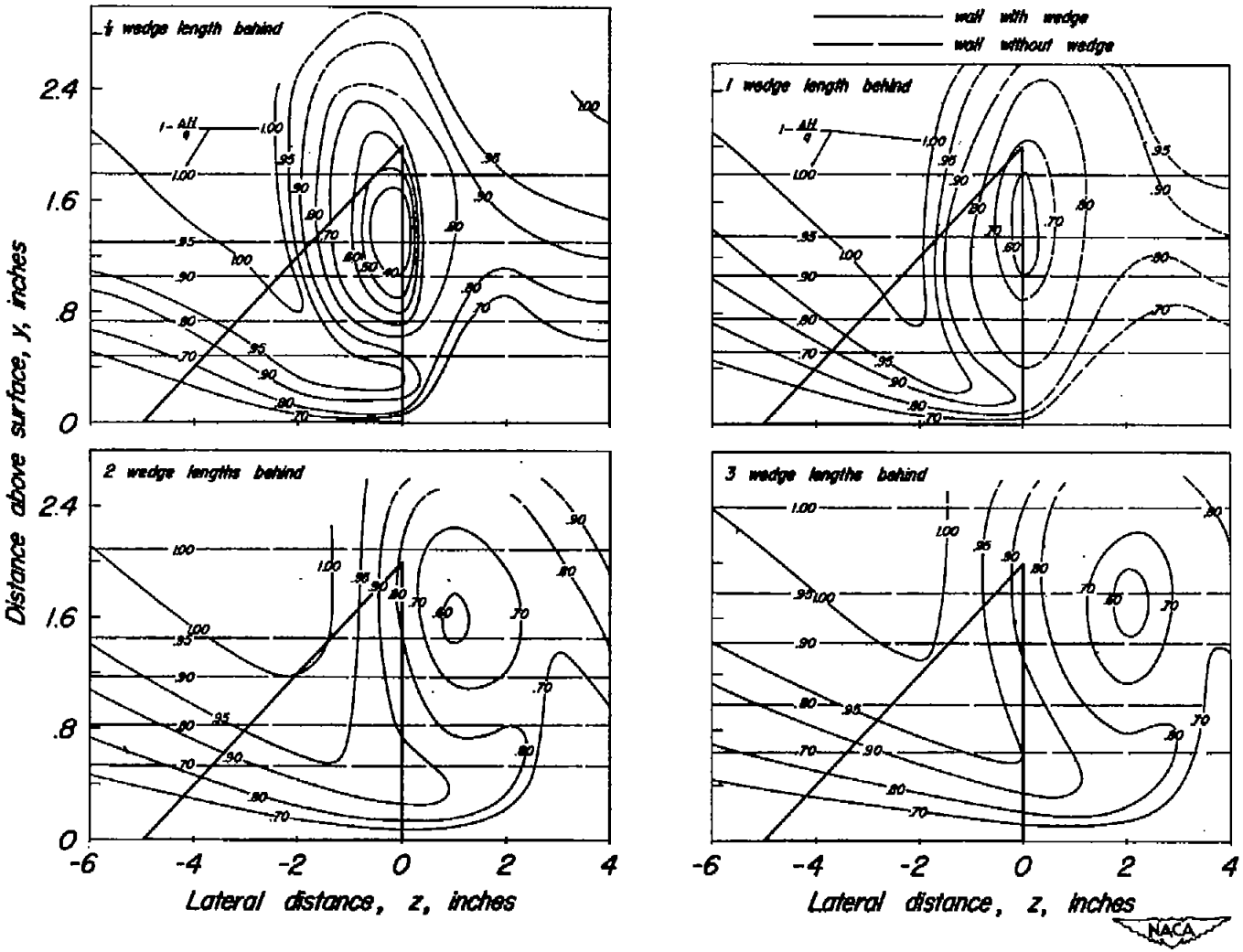

Figure 6.-Total-pressure contours downstream of a wedge mounted on the dummy wall. (Contours viewed looking upstream toward wedge.)

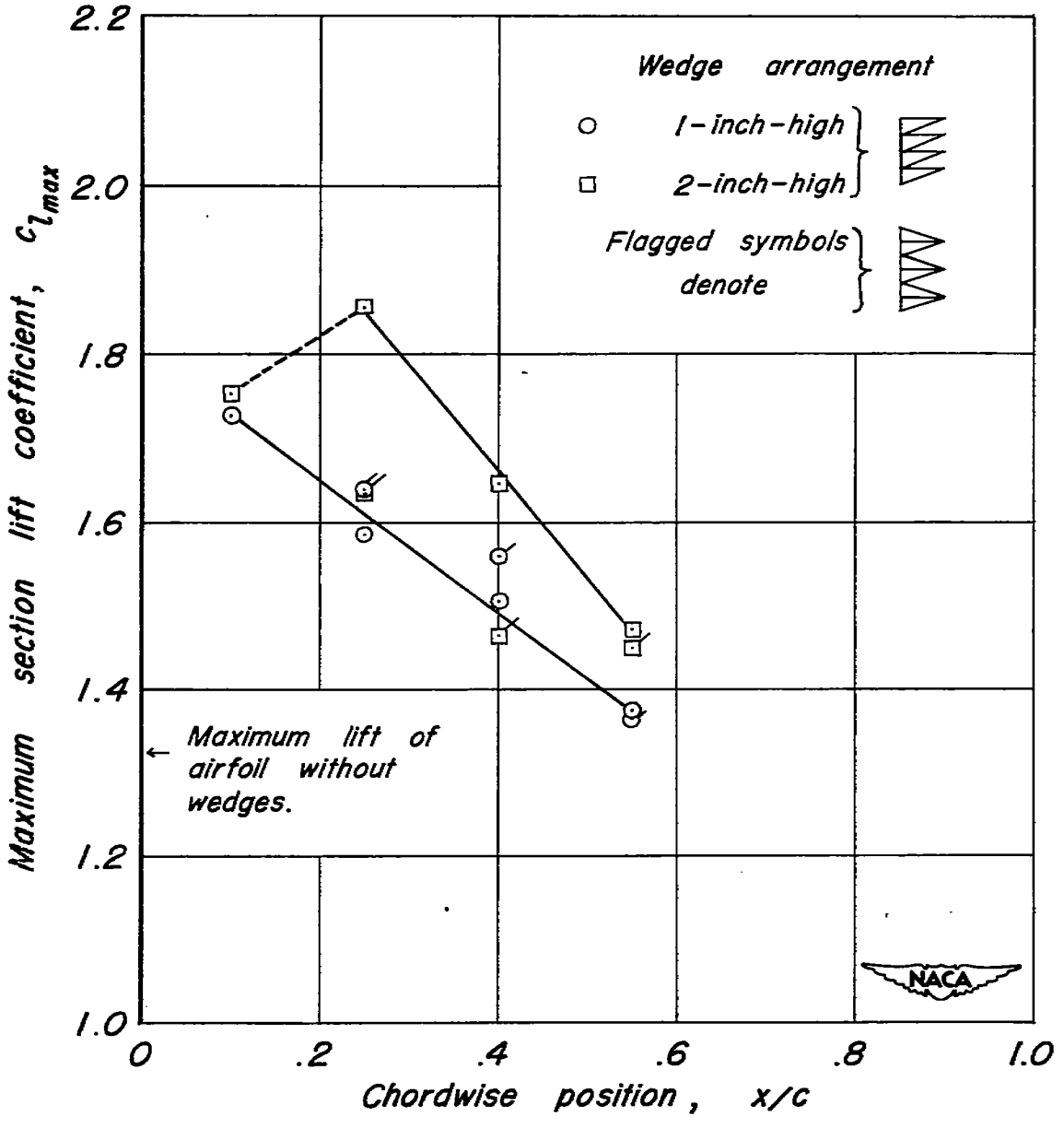

Figure 7.- Variation of maximum lift with chordwise position of leading edges of adjoining wedges.

[redacted]

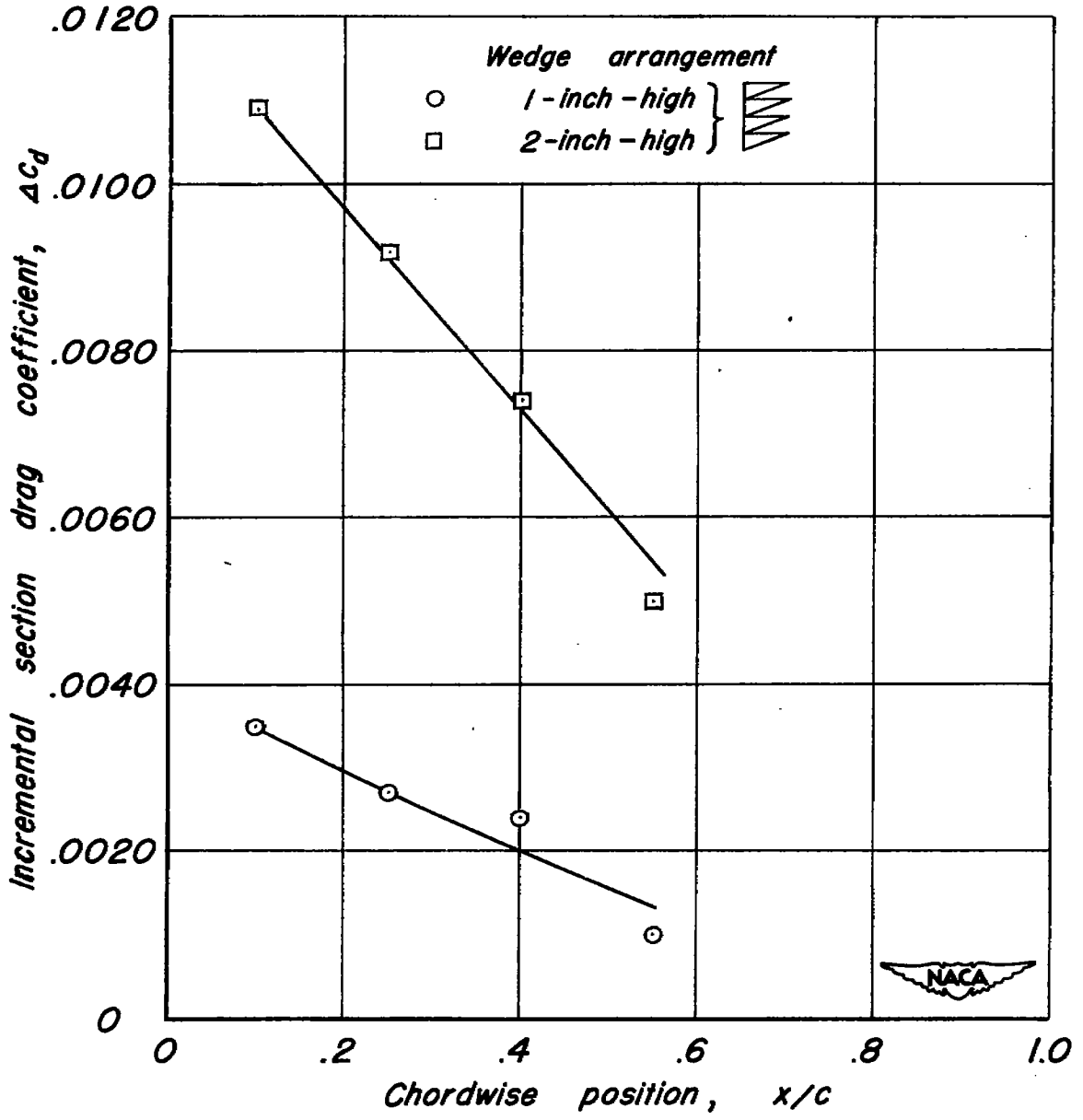

Figure 8.— Variation of incremental drag at zero lift with chordwise position of leading edges of adjoining wedges.

[redacted]

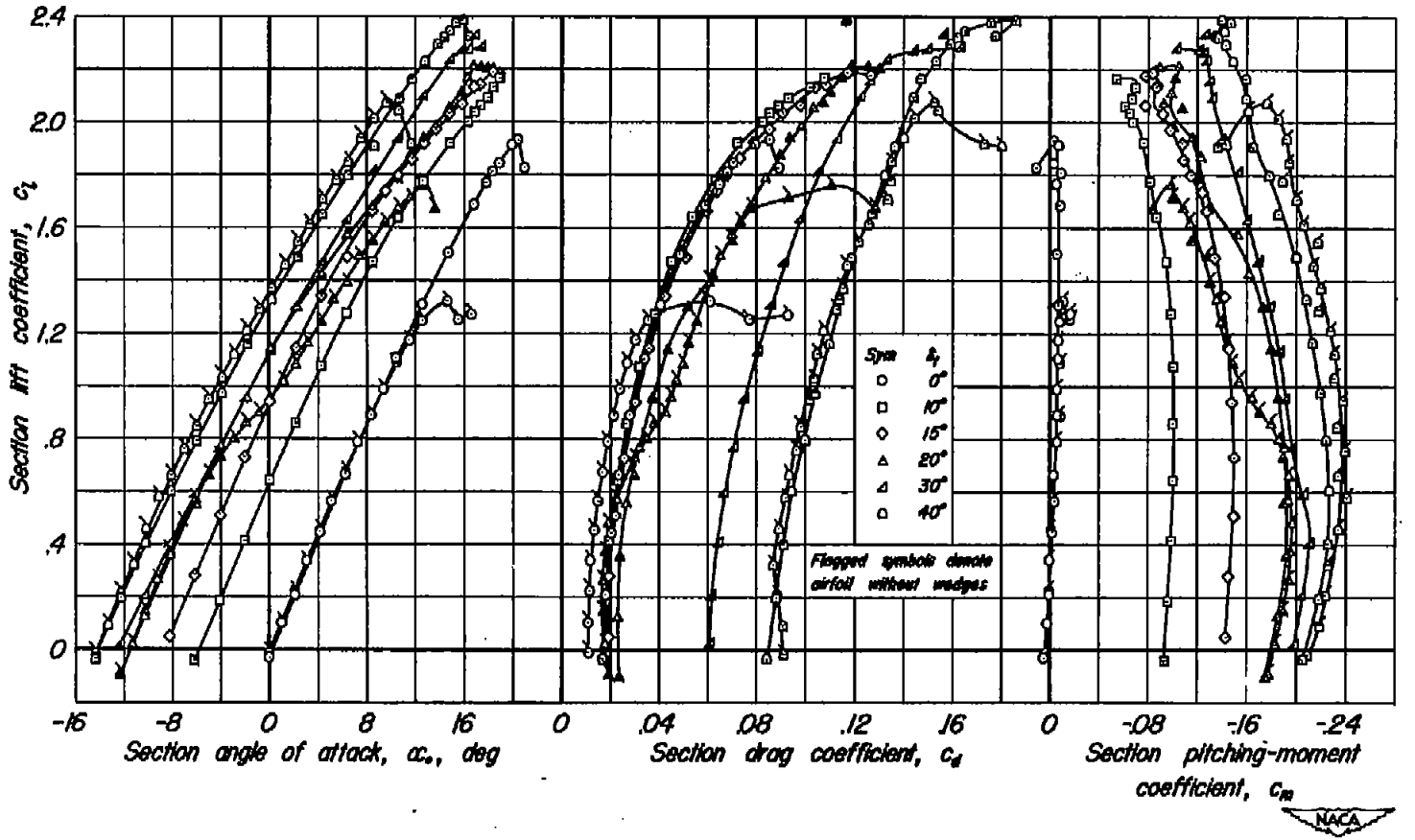

Figure 9.- Lift, drag, and pitching-moment characteristics of the NACA 63_3-018 airfoil section with and without wedges.

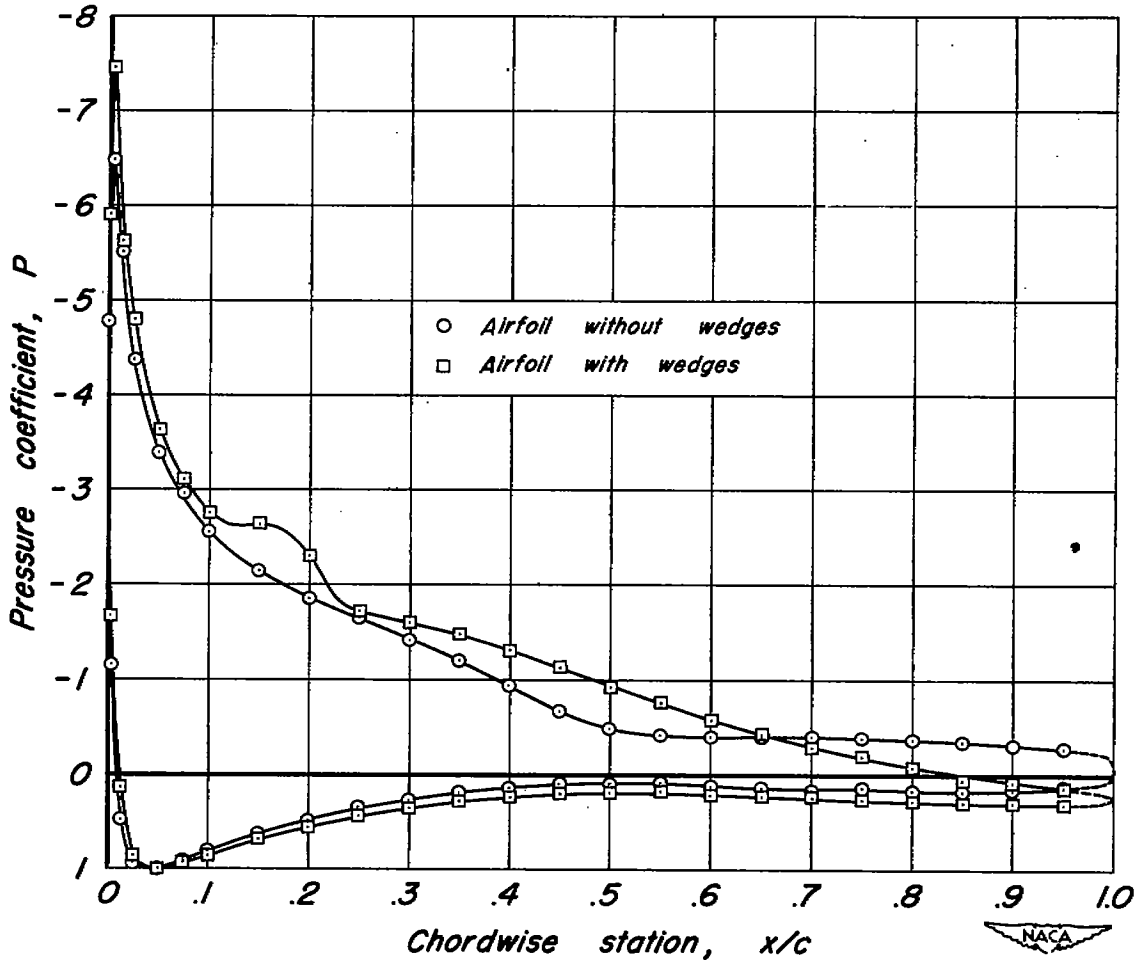

Figure 10.– Pressure distribution on the NACA 63_3-018 airfoil section with and without wedges. α_o, 14.7°.

[redacted]

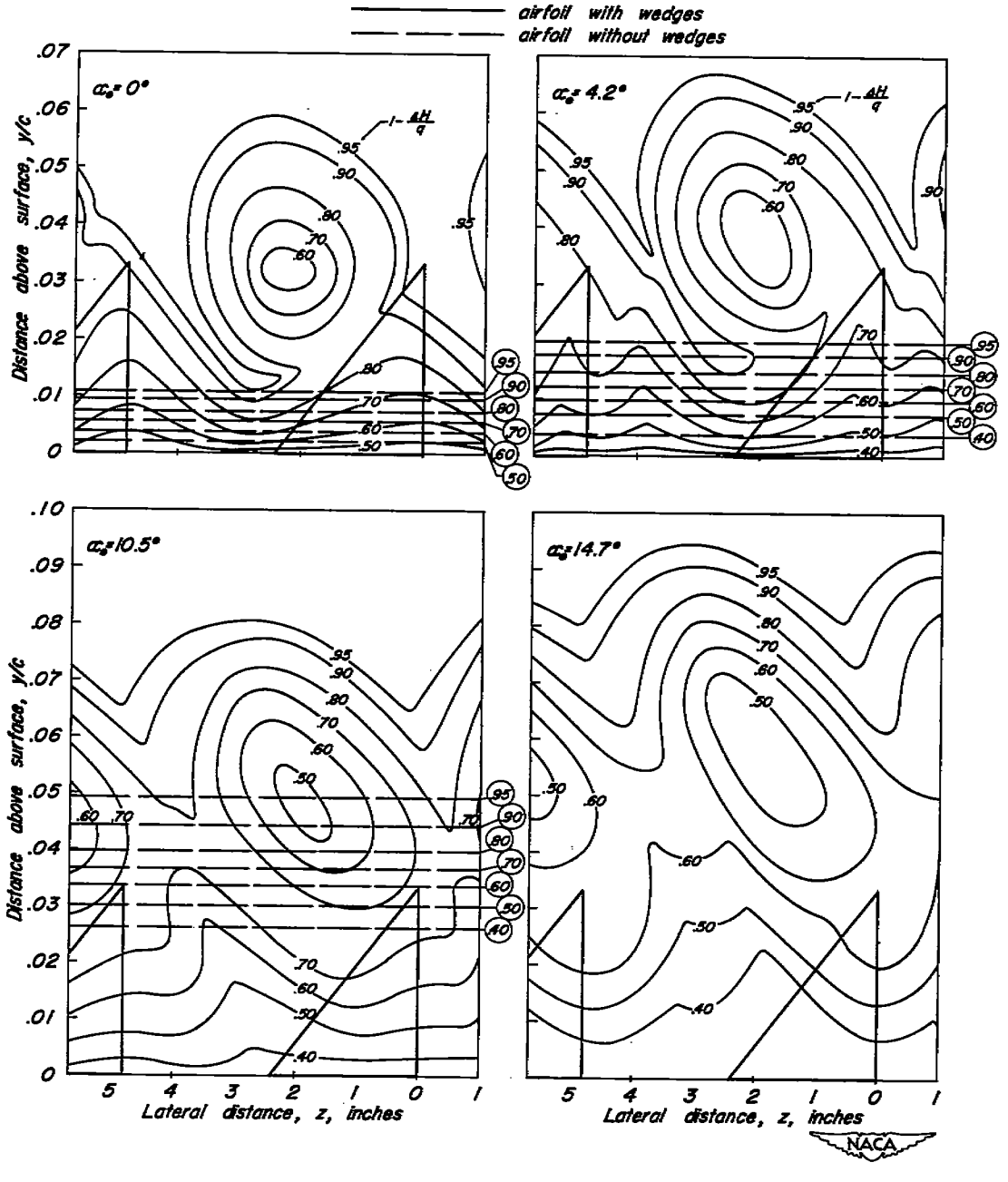

Figure 11.– Total-pressure contours at 95-percent chord for the NACA 63_3-018 airfoil model.

[redacted]

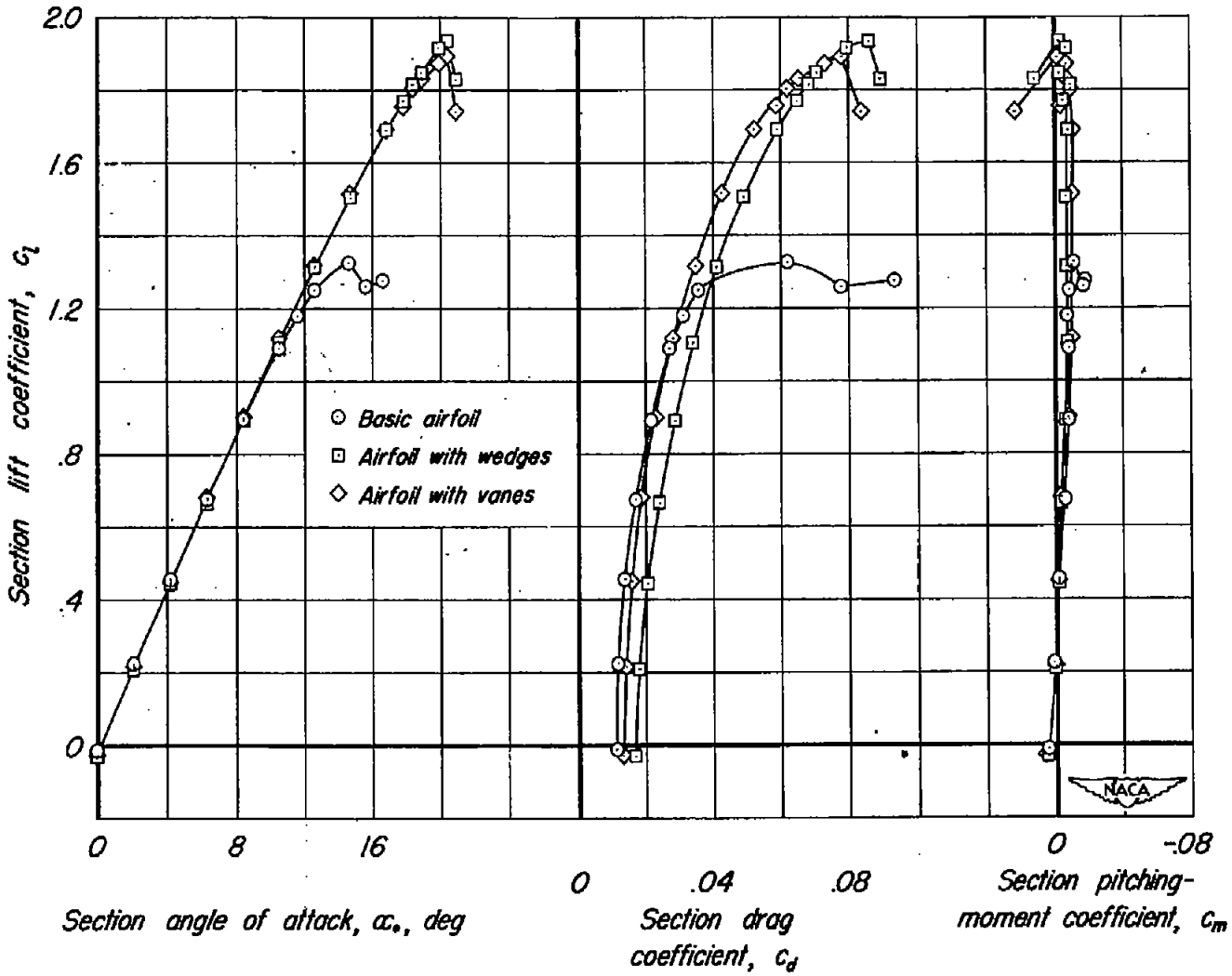

Figure 12.- Comparison of force characteristics for the airfoil with wedges and with vanes.